



LAWRENCE
LIVERMORE
NATIONAL
LABORATORY

Microscopic theory of thermoelectric properties of silicon nanowires

T. Vo, A. Williamson, V. Lordi, G. Galli

October 22, 2008

Nano Letters

Disclaimer

This document was prepared as an account of work sponsored by an agency of the United States government. Neither the United States government nor Lawrence Livermore National Security, LLC, nor any of their employees makes any warranty, expressed or implied, or assumes any legal liability or responsibility for the accuracy, completeness, or usefulness of any information, apparatus, product, or process disclosed, or represents that its use would not infringe privately owned rights. Reference herein to any specific commercial product, process, or service by trade name, trademark, manufacturer, or otherwise does not necessarily constitute or imply its endorsement, recommendation, or favoring by the United States government or Lawrence Livermore National Security, LLC. The views and opinions of authors expressed herein do not necessarily state or reflect those of the United States government or Lawrence Livermore National Security, LLC, and shall not be used for advertising or product endorsement purposes.

Microscopic theory of thermoelectric properties of silicon nanowires

Trinh Vo,^{1,*} Andrew J. Williamson,¹ Vincenzo Lordi,¹ and Giulia Galli²

¹Lawrence Livermore National Laboratory, Livermore, CA 94550

²University of California, Davis, CA 95616

We present predictions of the thermoelectric figure of merit (ZT) of Si nanowires, as obtained using Boltzman transport equation and *ab-initio* electronic structure calculations. We find that ZT is strongly dependent on the nanowire growth direction and surface reconstruction and we discuss general rules to select silicon based nanostructures with combined n-type and p-type optimal ZT. In particular, our calculations indicate that 1 nm wires grown in the [001] and [011] directions can attain ZT values which are about twice as high as those of ordinary thermoelectric materials.

Recent progress in nanomaterials synthesis has enabled the growth of semiconducting nanowires (NWs) with a range of sizes, growth directions, and surface structures. [1–4] These wires exhibit a strong size dependence of their electronic and optical properties [5–8], and are attractive candidates for photovoltaic devices, photodetectors, field-effect transistors [9, 10], inverters, [11] light-emitting diodes and nano-scale sensors. [12, 13]

Among the numerous potential applications of silicon NW, recent studies have focused on their promise as thermoelectric (TE) materials with a so called improved figure of merit (ZT) [14–16]. The suitability of a system to convert heat into electricity or electricity into heat is usually quantified in terms of ZT, which is defined as:

$$ZT = \sigma \frac{TS^2}{\kappa_e + \kappa_l} . \quad (1)$$

Here S is the Seebeck coefficient, σ is the electronic conductivity, and κ_e, κ_l are the electronic and lattice contributions to the thermal conductivity.

For several decades, many investigations have focused on the search for materials with a high TE figure of merit, but it has been extremely challenging to find any system with ZT higher than 1 [17]. Recent experimental studies have suggested that the value of ZT can be significantly increased by incorporating nanostructures into bulk materials. [18]. In particular, it has been proposed that at the nanoscale, quantum confinement may provide a mechanism for engineering systems with reduced electron and hole masses, and hence increased mobilities, which in turn could lead to increased values of the electrical conductivity. Additionally, at the nanoscale the large surface to volume ratio may increase the scattering of phonons by the surface, thus decreasing the thermal conductivity (κ_l), compared to bulk values, and increasing the TE figure of merit. [16, 19–25]. However, a mere size reduction and possible decrease in effective masses do not necessarily lead to an improved figure of merit; indeed quantum confinement is expected to increase surface scattering of electrons, which would lead to a reduction of σ . Therefore, predicting nanoscale effects on thermoelectric properties requires quantitative calculations of σ , κ_e , κ_l , and S for specific systems, and a thorough understanding of

how electronic properties determine these transport coefficients, whose values are inter-dependent in a complex manner.

In this Letter, we report on atomistic calculations of the thermoelectric figure of merit of silicon nanowires (SiNW), a prototypical, nanostructured material for thermoelectric applications. A combination of Molecular Dynamics (MD) simulations, Density Functional Theory (DFT) structural and electronic calculations, and Boltzmann Transport Equation (BTE) simulations are used to provide a microscopic theory of thermoelectric properties of silicon nanowires and to predict how to design silicon based materials with improved ZT.

We studied hydrogen terminated SiNWs grown along the [001], [011] and [111] directions, with diameters of 1.1-1.2 nm, and surfaces with canted SiH₂ dihydrides and (2x1) reconstructed surfaces. In a previous work [26] we showed that SiNW with surfaces terminated by symmetric SiH₂ dihydrides are metastable, therefore we do not consider those geometries here. Figure 1 shows side views of the SiNWs for each growth direction (Fig. 1a) and the two surface structures (Fig. 1b) considered in this work. The relaxed atomic and band structures for each SiNW were calculated using DFT following the procedure described in Ref.[26]. Having obtained the band structure, electronic energies and velocities, the electrical conductivity σ , the electronic contribution to the thermal conductivity, κ_e , and the Seebeck coefficient, S , were obtained from the solution of the one dimensional Boltzman Transport Equation (BTE) in the constant-relaxation-time approximation (RTA):

$$\begin{aligned} \sigma &= \Lambda^{(0)}, \\ \kappa_e &= \frac{1}{e^2 T} [\Lambda^{(2)} - \Lambda^{(1)} (\Lambda^{(0)})^{-1} \Lambda^{(1)}], \\ S &= \frac{1}{e T} (\Lambda^{(0)})^{-1} \Lambda^{(1)} \quad , \quad \text{where} \\ \Lambda^{(\alpha)} &= e^2 \tau \int \frac{d\mathbf{k}}{\pi} \left(-\frac{\delta f}{\delta \varepsilon} \right) v(\mathbf{k}) v(\mathbf{k}) (\varepsilon(\mathbf{k}) - \mu)^\alpha \quad (2) \end{aligned}$$

Here e is the charge of carriers, T is the temperature, $f(\varepsilon)$ is the Fermi distribution function, $\varepsilon(\mathbf{k})$ is the energy associated with a given wave vector \mathbf{k} , τ is the relaxation time, $v(\mathbf{k})$ is the group velocity, and μ is the electronic

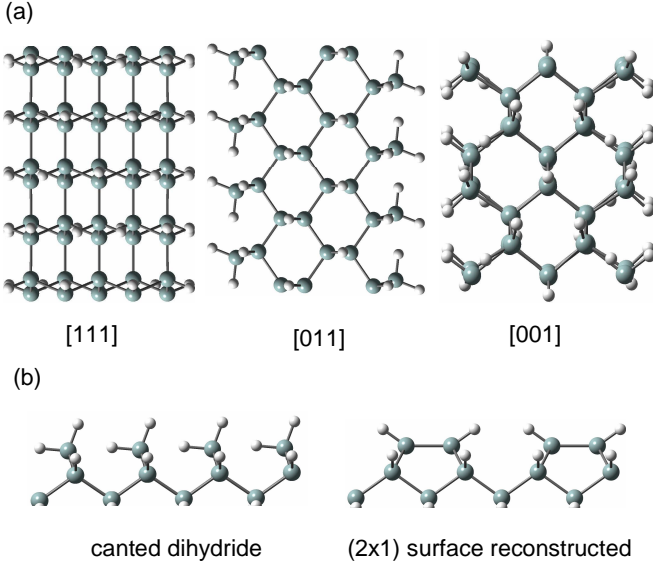


FIG. 1: (Color online) Fully relaxed 1.1 nm Si NWs: (a) in three different growth directions [001], [011], and [111], and (b) with two different surface geometries.

chemical potential. The velocity $v(\mathbf{k})$ is calculated from the band structure:

$$v = \frac{1}{\hbar} \frac{\delta \varepsilon(\mathbf{k})}{\delta \mathbf{k}} \quad (3)$$

We assumed that transport in SiNWs occur in a diffusive regime, and σ , S , and κ_e were evaluated by considering only elastic scattering processes. Inclusion of non-elastic scattering would call for the use of approaches beyond the RTA. We note that Gilbert *et al.*, [27] have recently suggested that transport is expected to switch from ballistic to diffusive in SiNWs longer than 1.4 nm. The wires considered here represent macroscopically long wires, as periodic boundary conditions in the wire growth direction were used in our calculations.

The relaxation time, τ , is a complex function of the atomic structure, electron energy, temperature, and carrier concentrations $\tau = \tau(\varepsilon, T)$. In systems with low doping and low carrier concentrations, τ is limited by phonon scattering. For high doping and carrier concentrations, τ is limited by impurity scattering. The goal of our work is to determine the effect of a SiNW's growth direction and surface structure on its TE figure of merit. Therefore, the values of τ were obtained by fitting σ values, calculated using Eq.(2), to experimentally measured, carrier concentration dependent mobility data.[28]

Fig. 2 shows the calculated σ , κ_e , S , and ZT , as a function of carrier concentration for p- and n-type 1.1 nm SiNWs with different growth directions, at 300K. Values of the lattice contribution to the thermal conductivity were obtained by using molecular dynamics calculations, and they will be discussed in detail elsewhere [29]. For 1 nm wire with pinned surfaces (which best represent rough

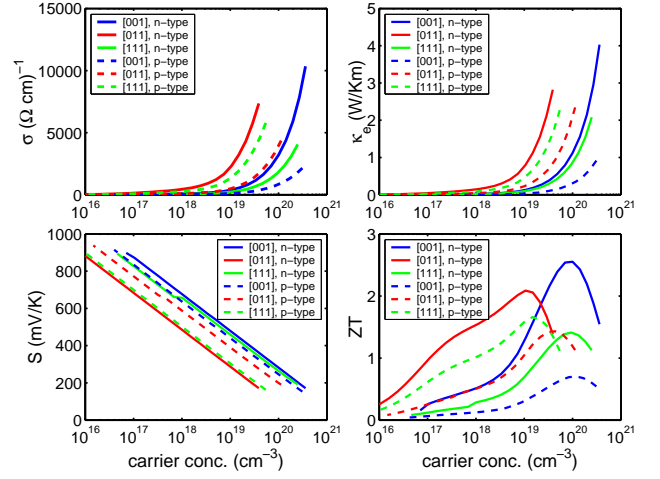


FIG. 2: (Color online) Calculated σ , κ_e , S , and ZT of p-type (dashed lines) and n-type (solid lines) doped 1.1 nm SiNWs grown along the [001], [011], and [111] directions.

surfaces obtained experimentally), we obtained values of about 2.0 W/mK, that are close to the experimental data recently reported for NWs with larger diameters [30] and to those computed in Ref. [31]. The carrier concentration n , is defined as $n = \int d\varepsilon N(\varepsilon) f(\varepsilon)$, where $N(\varepsilon)$ is the electronic density of states. In this model, n represents the concentration of charge carriers in a system which is artificially doped by varying the chemical potential, while assuming a fixed band structure.

Figure 2 shows that as the concentration of electrons or holes increases, both σ and κ_e increase as more carriers are available to transport both charge and heat, while the Seebeck coefficient decreases with increasing carrier concentration. In addition to a dependence on carrier concentration, σ , κ_e , and S also show a strong dependence on growth direction arising from differences in the band structure. For SiNWs grown in the [011] direction, the conduction band minimum (CBM) is highly dispersive, and the electronic states are delocalized in the direction parallel to the SiNW axis. In contrast, the CBMs in the [001] and [111] SiNWs are oriented in the direction diagonal and perpendicular to the NW axis, respectively, and the band structures are much flatter (see Ref. [26]). Consequently, the [011] SiNWs have the lowest effective mass and highest values of σ and κ_e for a given carrier concentration. Therefore, if one is only interested in selecting wires with the highest electrical conductivity, our simulations predict that the [011] growth direction is the most promising.

However, for TE materials, the challenge is not simply to maximize the electrical conductivity, but to engineer an electronic band structure which maximizes the TE figure of merit (see Eq. 1). Figure 2 shows that ZT initially increases with carrier concentration as σ increases. At higher carrier concentrations, the increase of κ_e and de-

crease of S result in a net decrease of ZT . Therefore, for a given growth direction and type of doping, there is an optimal carrier concentration which yields the maximum attainable value of ZT . For the 1.1 nm wires shown in Fig. 2, these optimal carrier concentrations vary between 10^{18} and 10^{20} cm^{-3} , producing maximum ZT values ranging from 0.6 to 2.6. These results demonstrate that nanoscale confinement, together with the choice of specific geometries at the microscopic scale, may be used to dramatically enhance the ZT value of silicon, compared to its bulk value of 0.02.

The values of ZT shown in Fig. 2 are likely to represent a lower bound to the actual ZT of a NW, as the τ values are fitted to bulk experimental mobilities and those of a nanometer sized wire are expected to be larger than in the bulk. In order to estimate the difference in mobilities between NWs and the bulk, we performed *ab-initio*, DFT calculations of scattering rate for representative samples of boron doped bulk Si and of a 1.1 nm NW (with a carrier concentration of $\sim 8 \times 10^{20}$ cm^{-3} and B in the interior of the NW). We followed the procedure outlined in Ref.[32]. For constant τ , one has: $\tau^{-1} \propto |T|^2 \cdot \text{DOS}$, where $|T|$ is a scattering matrix element and DOS is the joint density of states for the transition contributing to $|T|$. We found that intra-valley scattering at the band extrema is dominant for both the NW and the bulk, and we therefore approximated $|T|$ with its value at the band extremum, using the Born approximation, and we calculated the average DOS over $5k_B T$ (here T is the temperature and k_B the Boltzmann constant). We obtain $\tau_{\text{wire}}/\tau_{\text{bulk}} \approx 1 - 4$, thus confirming the intuitive expectation of larger relaxation times in a small nanowire, with respect to bulk values.

When selecting an optimal growth direction for a TE material constructed from SiNWs, one should also consider the level of doping required to achieve a given ZT value. For example, [001] SiNWs have a higher n-type ZT value of 2.6 compared to 2.1 for [011] direction; however a carrier concentration of 1×10^{20} cm^{-3} is required to achieve it, compared to only 1×10^{19} cm^{-3} for the [011] case. Given that the maximum doping concentration obtainable in bulk Si is of the order of 10^{21} cm^{-3} , reaching a doping level of 10^{20} cm^{-3} in a 1 nm SiNW may be challenging. Therefore, from a practical point of view, the [011] growth direction is probably the best candidate for TE materials.

To produce a TE device, one needs to combine p- and n-type wires into a parallel structure, such as that proposed by Mujamdar *et al.* in Ref. [18]. The maximum overall ZT for such a structure can be obtained by using NWs with appropriate doping types (n- or p-type), concentration, and growth direction. For instance, combining the n-type [011] with a doping concentration corresponding to the max ZT (1×10^{19}) and p-type [111] with a doping concentration of 3×10^{19} will yield a device ZT value of 1.9 (see Fig. 2).

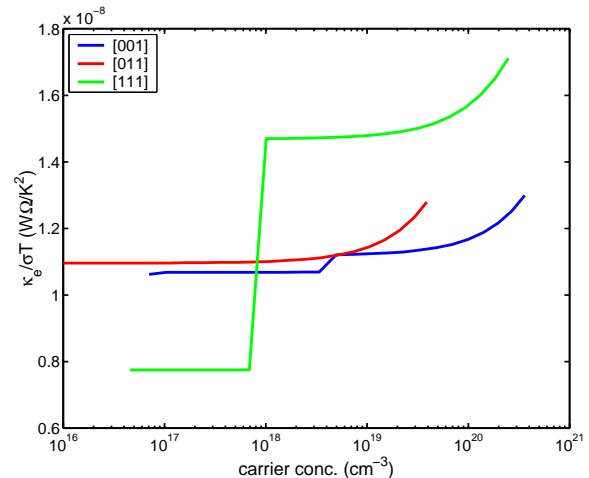


FIG. 3: (Color online) Lorentz number as a function of carrier concentration, n for SiNWs with [001], [011], and [111] growth directions.

More insight into the dependence of ZT on carrier concentration can be gained from examining the *ratio* of the electronic to thermal conductivity, i.e. the Lorentz number, $\kappa_e/\sigma T$. Figure 3 shows a plot of the Lorentz number as a function of electron concentration for n-type SiNWs for three different growth directions. This number depends on the details of the band structure. Eq. (2) shows that while the electronic conductivity, σ , depends only on the velocity of carriers at a given \mathbf{k} -point, $v(\mathbf{k})$, the electronic contribution to thermal conductivity also depends on the energy transported by a carrier at that \mathbf{k} -point, $\epsilon(\mathbf{k})$. Therefore, the magnitude of energy gaps within the conduction band will affect how doping can be achieved and thus the values of the electronic contribution to the thermal conductivity. For example, when the carrier concentration increases above 1×10^{18} the second lowest conduction band in the [111] wire becomes occupied. This second band has a relatively low electron velocity, and it makes only a small additional contribution to the electronic conductivity. However, the higher energy, $\epsilon(\mathbf{k})$, of this second band makes a larger contribution to the electronic component of the thermal conductivity, κ_e , and a sharp increase in the Lorentz number is observed. Therefore, when designing an optimal thermoelectric device, one needs to extend the standard concept of band-gap-engineering to band structure-engineering, where several energy splittings in the conduction bands of the systems are also optimized.

Finally, in addition to examining the dependence of the figure of merit ZT on growth direction, we also examine its dependence on the surface structure of the SiNWs. Figure 4 compares the carrier dependence of ZT for n-type SiNWs with canted dihydride and (2x1) reconstructed surface structures. The NW diameter of 1.2nm is used for the case of [111], since NWs with smaller diam-

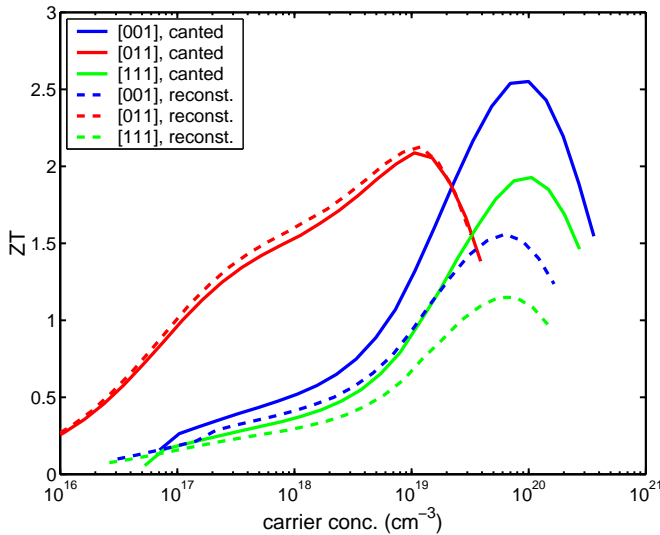


FIG. 4: (Color online) The figure of merit as a function of carrier concentration for n-type SiNWs with two different surface structures and the three growth directions [001], [011], and [111]. The NW diameter is 1.2nm for [111] direction and 1.1nm for others.

eters do not have surface reconstruction. For [001] and [111] wires, the surface reconstruction produces a small band splitting at the conduction band minimum. [26] This results in a partial occupation of the higher energy bands, resulting in a smaller value of κ_e and hence a smaller maximum value of ZT . In the case of [011] wires, there is a large splitting between the first and second conduction bands, for both canted and reconstructed surface, so the maximum value of ZT is relatively unaffected by the surface reconstruction. These results again emphasize the need to optimize not only the band gap, but also band splittings and effective masses of a given material, in order to optimize its value of ZT .

In conclusion, we have employed a combination of first-principles electronic structure and Boltzmann transport calculations to predict the thermoelectric figure of merit of silicon nanowires. Our results show that SiNWs are good candidates for fabricating thermoelectric materials. We predict a lower bound for the combined n- and p-type figures of merit, as high as 2, which is two orders of magnitude larger than that of bulk silicon. By changing the growth direction and NW diameter, or by tuning the surface structure via chemical etching or heat treatment, it is possible to engineer SiNWs with a wide range of technologically important electronic and thermoelectric properties. In principle, it should also be possible to further optimize NW thermoelectric properties by alloying silicon with other elements, such as germanium, and we are currently investigating this possibility.

We would like to thank John Reed for performing the Molecular Dynamics simulation of the lattice conductivity, κ_l , and Eric Schwegler for useful discussion.

This work was performed under the auspices of the U.S. Department of Energy by the University of California, Lawrence Livermore national laboratory under Contract No. W-7405-Eng-48. This work was supported by DARPA grant W911NF-06-1-0175.

* Electronic address: vo4@llnl.gov

- [1] S. Sharama, T. Kamin, and R. Williams, *Appl. Phys. A* **80**, 1225 (2005).
- [2] Y. Zhang, Y. Tang, N. Wang, C. Lee, I. Bello, and S. Lee, *J. Crys. Grow.* **197**, 136 (1999).
- [3] X. Yan, D. Liu, L. Ci, J. Wang, Z. Zhou, H. Yuan, L. Song, Y. Gao, L. Liu, W. Zhou, et al., *J. Crys. Grow.* **257**, 69 (2003).
- [4] A. Hochbaum, R. Fan, R. He, and P. Yang, *Nano Lett.* **5**, 457 (2005).
- [5] L. Canham, *Appl. Phys. Lett.* **57**, 1046 (1990).
- [6] D. Katz, T. Wizansky, and O. Milo, *Phys. Rev. Lett.* **89**, 86801 (2002).
- [7] X. Duan, J. Wand, and C. Lieber, *Appl. Phys. Lett.* **76**, 1116 (2000).
- [8] D. Ma, C. Lee, C. Au, S. Tong, and S. Lee, *Science* **299**, 1874 (2003).
- [9] X. Duan, Y. Huang, Y. Cui, J. Wang, and C. Lieber, *Nature* **409**, 66 (2001).
- [10] Y. Cui, Z. Zhong, D. Wang, W. Wang, and C. Lieber, *Nano Lett.* **3**, 149 (2003).
- [11] Y. Cui and C. Lieber, *Science* **291**, 851 (2001).
- [12] J. Hahn and C. Lieber, *Nano Lett.* **4**, 51 (2004).
- [13] Y. Cui, Q. Wei, H. Park, and C. Lieber, *Science* **293**, 1289 (2001).
- [14] A. Abramson, W. Kim, S. Huxtable, H. Yan, Y. Wu, A. Majumdar, C. Tien, and P. Yang, *J. Microelectromech. Sys.* **13**, 505 (2004).
- [15] M. Dresselhaus, G. Dresselhaus, X. Sun, Z. Zhang, S. Cronin, and T. Koga, *Phys. Sol. State* **41**, 679 (1999).
- [16] S. Kubakaddi and B. Mulimani, *J. Appl. Phys.* **58**, 3643 (1985).
- [17] A. Majumdar, *Science* **303**, 777 (2004).
- [18] A. Majumdar, *J. Microelectromech. Sys.* **13**, 505 (2004).
- [19] L. Hicks, *Appl. Phys. Lett.* **63**, 3230 (1993).
- [20] L. Hicks and M. Dresselhaus, *Phys. Rev. B* **47**, 16631 (1993).
- [21] X. Sun, Z. Zhang, and M. Dresselhaus, *Appl. Phys. Lett.* **74**, 4005 (1999).
- [22] O. Rabin, Y. Lin, and M. Dresselhaus, *Appl. Phys. Lett.* **79**, 81 (2001).
- [23] A. Khitun, A. Balandin, and K. Wang, *Superlattices Microstructures* **26**, 181 (1999).
- [24] L. Hicks and M. Dresselhaus, *Phys. Rev. B* **47**, 12727 (1993).
- [25] L. Hicks, T. Harman, X. Sun, and M. Dresselhaus, *Phys. Rev. B* **53**, 10493 (1996).
- [26] T. Vo, A. Williamson, and G. Galli, *Phys Rev B* **74**, 045116 (2006).
- [27] M. Gilbert, R. Akis, and D. Ferry, *J. Appl. Phys.* **98**, 094303 (2005).
- [28] C. Jacoboni, C. Canali, G. Ottaviani, and A. Quaranta, *Solid State Electron* **20**, 77 (1977).
- [29] J. Reed, A. J. Williamson, and G. Galli, To be published

- (2007).
- [30] A. Hochbaum, R. Chen, R. D. Delgado, E. Garnett, A. Majumdar, and P. Yang, Private communication (2007).
- [31] N. Mingo, L. Yang, D. Li, and A. Majumdar, Nano Lett. **3**, 1713 (2003).
- [32] M. H. Evans, X.-G. Zhang, J. D. Joannopoulos, and S. T. Pantelides, Phys. Rev. Lett. **95**, 106802 (2005).